FACTORIZABLE ELECTROWEAK ONE-LOOP CORRECTIONS TO TOP QUARK PAIR PRODUCTION AND DECAY IN e^+e^- COLLISIONS* **

Karol Kołodziej†, Adam Staroń‡

Institute of Physics, University of Silesia
Uniwersytecka 4, 40-007 Katowice, Poland

(Received November 2, 2005)

We discuss an influence of the quantum electrodynamics corrections due to the initial state radiation in the structure function approach and factorizable electroweak $\mathcal{O}(\alpha)$ corrections in the pole approximation on the standard model predictions for top quark pair production and decay into six fermions at a linear e^+e^- collider. The discussion is illustrated with numerical results for one selected six-fermion reaction $e^+e^- \to b\nu_\mu\mu^+\bar{b}\mu^-\bar{\nu}_\mu$.

PACS numbers: 12.15.Lk, 13.40.Ks, 14.65.Ha

1. Introduction

The process of top-quark pair production

$$e^+e^- \to t\bar{t} \tag{1}$$

at the future e^+e^- International Linear Collider (ILC) [1] will be measured as a dominant contribution to six-fermion reactions of the form

$$e^+e^- \to bf_1\bar{f}_1'\bar{b}f_2\bar{f}_2', \tag{2}$$

where $f_1, f_2' = \nu_e, \nu_\mu, \nu_\tau, u, c$ and $f_1', f_2 = e^-, \mu^-, \tau^-, d, s$. How the top quark pair production contributes to reactions (2) is illustrated in Fig. 1(a), where

* Presented by K. Kołodziej at the XXIX International Conference of Theoretical Physics, "Matter to the Deepest", Ustroń, Poland, September 8–14, 2005. Based on work in collaboration with Alejandro Lorca and Tord Riemann.

** Work supported in part by the Polish State Committee for Scientific Research (KBN) in years 2005–2007 as a research grant.

† kolodzie@us.edu.pl

‡ staron@server.phys.us.edu.pl

the two dominant 'signal' Feynman diagrams which contain two resonating top-quark propagators are shown. On the other hand, the diagrams depicted in Fig. 1(b) and 1(c) are examples of many other, typically several hundred, Feynman diagrams which also contribute to (2) already in the lowest order of the standard model (SM). As these diagrams contain either one or none top quark propagator, they constitute the off resonance background contribution to the top quark pair production.

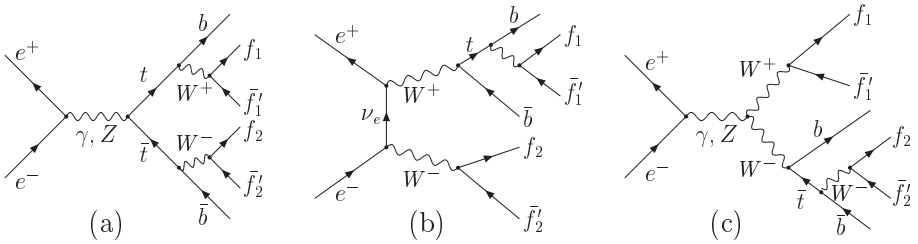

Fig. 1. Examples of Feynman diagrams of reaction (2): (a) "signal", (b) and (c) "background" diagrams.

As measurements of the top quark pair production at the ILC are expected to reach a very high precision level of 1%, or even higher, the SM theoretical predictions are supposed to match that high precision level. This obviously requires taking into account radiative corrections in the predictions for the six fermion reactions (2). The task of calculating full electroweak (EW) $\mathcal{O}(\alpha)$ correction to any of reactions (2) does not seem to be solvable at present, mainly because of 8 external particles and a large number of the contributing Feynman diagrams. For example, in the unitary gauge, with neglect of the Higgs boson couplings to fermions lighter than a b-quark, reactions $e^+e^- \to b\nu_\mu\mu^+\bar{b}d\bar{u}$, $e^+e^- \to b\nu_\mu\mu^+\bar{b}\mu^-\bar{\nu}_\mu$, and $e^+e^- \to bu\bar{d}\bar{b}d\bar{u}$ get contributions from 264, 452, and 1484 Feynman diagrams, respectively.

In this lecture, we will discuss an alternative simplified approach to the problem of improving precision of the SM lowest order predictions for (2) that has been first proposed in [2] and recently accomplished in [3].

2. Calculation scheme

The approach developed in [3] relies on an observation that the double-resonant signal contribution, represented by the diagrams of Fig. 1(a), dominates the lowest order total cross section of any channel of (2) in a wide range of the center of mass energies, starting from a few GeV above the top-pair production threshold up to the energies of a few TeV [4–6]. Therefore, it seems natural to include the factorizable EW $\mathcal{O}(\alpha)$ corrections just to the two 'signal' diagrams and to utilize a pole approximation, similar to that

which had been developed in the context of the W-boson pair production at LEP2 [7] and for the Higgsstrahlung at a linear collider [8], and the leading quantum electrodynamics (QED) corrections due to the initial state radiation (ISR) in the structure function approach. The corrections are included in the differential cross section for (2) according to the following master formula

$$d\sigma = \int_0^1 dx_1 \int_0^1 dx_2 \, \Gamma_{ee}^{\mathrm{LL}}(x_1, s) \, \Gamma_{ee}^{\mathrm{LL}}(x_2, s) \, d\sigma_{\mathrm{Born+FEWC}}(x_1 p_1, x_2 p_2) \; , \quad (3)$$

where $x_1 p_1$ ($x_2 p_2$) is the four momentum of the positron (electron) after emission of a collinear photon, $\Gamma_{ee}^{\mathrm{LL}}(x, s)$ is the structure function in the LL approximation which is given by Eq. (67) of [9], with `'BETA'` choice for non-leading terms and the splitting scale equal to $s = (p_1 + p_2)^2$, and $d\sigma_{\mathrm{Born+FEWC}}$ is the cross section including the factorizable EW $\mathcal{O}(\alpha)$ correction in the pole approximation. It is calculated at the reduced center of mass (CM) energy corresponding to $s' = x_1 x_2 s$, with the neglect of the electron mass, according to

$$d\sigma_{\mathrm{Born+FEWC}} = \frac{1}{2s'} \left\{ \overline{|M_{\mathrm{Born}}|^2} \; + 2 \, \mathrm{Re} \overline{\left(M_{t\bar{t}}^* \, \delta M_{t\bar{t},\mathrm{FEW}} \right)} \right\} d\Phi_{6f} \; , \quad (4)$$

where M_{Born} is the Born matrix element of reaction (2), $M_{t\bar{t}}$ and $\delta M_{t\bar{t},\mathrm{FEW}}$ is, respectively, the lowest order amplitude of the 'signal' Feynman diagram of Fig. 1(a) and the corresponding factorizable EW $\mathcal{O}(\alpha)$ correction, both in the pole approximation. The overlines in (4) denote, as usual, an initial state particle spin average and a sum over final state particle polarizations, and $d\Phi_{6f}$ is the Lorentz invariant six-particle phase space element.

The matrix element M_{Born} for a given channel of (2) is calculated with a program `eett6f` [10] taking into account a complete set of the lowest order Feynman diagrams. The corrections that we take into account in $\delta M_{t\bar{t},\mathrm{FEW}}$ are illustrated diagramatically in Fig. 2. The diagram in Fig. 2(a) represents the one-loop EW correction to the process of on-shell top-quark pair production (1), which is calculated numerically with a subroutine based on a program `topfit` [11]. The latter reproduces successfully results of both earlier [12] and more recent calculations [13] of the EW corrections to reaction (1). The EW one-loop corrections to the top- and antitop-quark decay are represented by the diagrams in Figs. 2(b) and 2(d), while the EW one-loop corrections to the W^+ and W^- decay are illustrated by the diagrams in Figs. 2(c) and 2(e). The decay corrections are calculated with newly written subroutines of `eett6f` which reproduce results for the EW one-loop corrected top-quark [14] and W-boson [15] decay widths. An interested

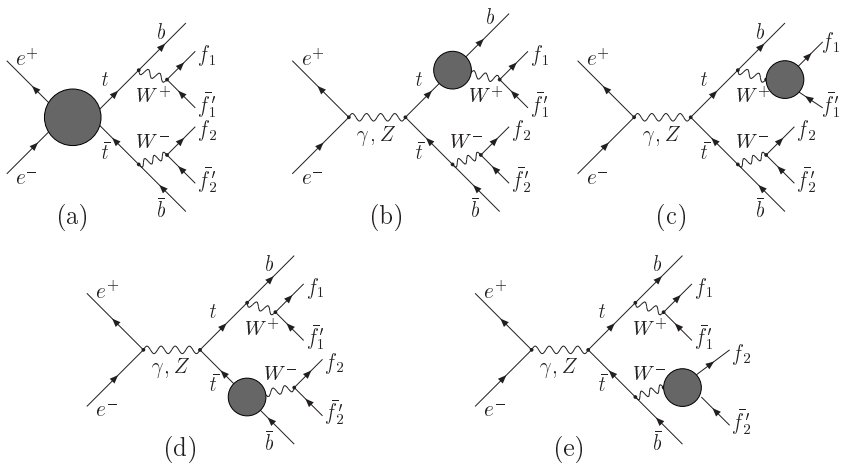

Fig. 2. Factorizable EW corrections to reaction (2).

reader is referred to [3] for the analytic form of these corrections and other details of the calculation. Here we recall only how the pole approximation is defined. It is obtained by the following replacements for the top-, antitop-quark and W-boson propagators in the amplitudes corresponding to the diagrams of Fig. 1(a) and Fig. 2

$$\frac{\not{p}+M_t}{p^2-M_t^2} \;\to\; \frac{\sum_\sigma u\,(p',\sigma)\otimes\bar{u}\,(p',\sigma)}{p^2-M_t^2}\,, \tag{5}$$

$$\frac{-\not{q}+M_t}{q^2-M_t^2} \;\to\; -\,\frac{\sum_{\bar{\sigma}} v\,(q',\bar{\sigma})\otimes\bar{v}\,(q',\bar{\sigma})}{q^2-M_t^2}\,, \tag{6}$$

$$\frac{-g_{\mu\nu}+\frac{k_\mu k_\nu}{M_W^2}}{k^2-M_W^2} \;\to\; \frac{\sum_\lambda \varepsilon_\mu\,(k',\lambda)\,\varepsilon_\nu\,(k',\lambda)}{k^2-M_W^2}\,, \tag{7}$$

where the spinors $u\,(p',\sigma)$ and $v\,(q',\bar{\sigma})$ of the top- and antitop-quark, and real polarization vectors $\varepsilon\,(k',\lambda)$ of the W^+ and W^- bosons are given in terms of the projected four momenta p', q' and k' which satisfy the on-shell relations $p'^2=q'^2=m_t^2$ and $k'^2=m_W^2$. They are obtained from the actual four momenta p, q and k of top-quark, antitop-quark and W-boson propagators with a projection procedure that has been described in [3]. In Eqs. (5) and (7), M_t and M_W are complex masses defined according to

$$M_t^2=m_t^2-im_t\Gamma_t, \qquad M_W^2=m_W^2-im_W\Gamma_W, \tag{8}$$

with the constant widths Γ_t and Γ_W introduced in order to regularize on-shell poles of the corresponding lowest order propagators. Substitution (8) is done only in the denominators of the corresponding lowest order propagators

and not in the one-loop amplitudes. Let us note that also the sums over the top-, antitop-quark and W-boson polarizations in the numerators of (5)–(7) result in real masses. However, this does not violate the substitution rule of (8), as substitutions (5)–(7) are done only in the factorizable one-loop correction term of (4).

The calculation of the EW factorizable corrections to reaction (2) in the pole approximation makes sense only if the invariant masses

$$m_{345} = \sqrt{(p_3+p_4+p_5)^2}, \qquad m_{678} = \sqrt{(p_6+p_7+p_8)^2} \tag{9}$$

of the $bf_1\bar{f}_1'$ and $\bar{b}f_2\bar{f}_2'$ are close to m_t each and if

$$m_{45} = \sqrt{(p_4+p_5)^2}, \qquad m_{78} = \sqrt{(p_7+p_8)^2} \tag{10}$$

of the $f_1\bar{f}_1'$ and $f_2\bar{f}_2'$ do not depart too much from m_W. Otherwise the signal diagrams of Fig. 1(a) stop to dominate the cross section and the association of the reduced phase space point, at which the EW factorizable $\mathcal{O}(\alpha)$ corrections depicted in Fig. 2 are calculated, with the phase space point of the full six particle phase space of (2) may lead to unnecessary distortion of the off resonance background contributions. Therefore in the following we will impose kinematical cuts on the quantities

$$\begin{aligned} \delta_t &= \frac{m_{345}}{m_t} - 1\,, \qquad \delta_{\bar{t}} = \frac{m_{678}}{m_t} - 1\,, \\ \delta_{W^+} &= \frac{m_{45}}{m_W} - 1\,, \qquad \delta_{W^-} = \frac{m_{78}}{m_W} - 1 \end{aligned} \tag{11}$$

which describe the relative departures of the invariant masses of (9) and (10) from m_t and m_W, respectively.

The 14-fold phase space integral in (4) is calculated numerically using a multichannel Monte Carlo approach, with the basic phase space parametrizations given by Eqs. (7)–(9) of [10].

3. Numerical results

We will illustrate the effect of the factorizable EW $\mathcal{O}(\alpha)$ corrections described in Section 2 on the SM predictions for six fermion reactions relevant for the top quark pair production and decay at the ILC by showing results for total cross sections for one specific channel of (2)

$$e^+e^- \to b\nu_\mu\mu^+\bar{b}\mu^-\bar{\nu}_\mu\,. \tag{12}$$

The numerical results presented here have been obtained with exactly the same values of the physical input parameters as in [3].

In Fig. 3, we plot the total cross section of reaction (12) as a function of the CM energy, to the lowest order and with inclusion of different classes of corrections in the presence of the following cuts on the quantities $\delta_t, \delta_{\bar{t}}, \delta_{W^+}, \delta_{W^-}$ defined in (11)

$$\delta_t < 0.1, \quad \delta_{\bar{t}} < 0.1\,, \qquad \delta_{W^+} < 0.1, \quad \delta_{W^-} < 0.1\,. \tag{13}$$

The dashed-dotted line shows the Born cross section, the dotted line is the cross section including the ISR correction, the dashed line shows an effect of the factorizable EW correction while the solid line shows an effect of the combined ISR and factorizable EW correction.

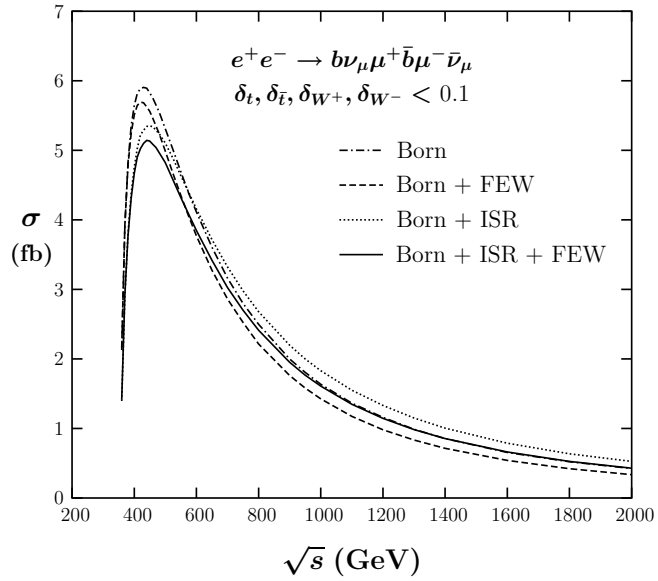

Fig. 3. Total cross sections of (12) including different classes of the SM radiative corrections as functions of the CMS energy.

The corresponding relative corrections

$$\delta_{\text{cor.}} = \frac{\sigma_{\text{Born+cor.}} - \sigma_{\text{Born}}}{\sigma_{\text{Born}}}, \qquad \text{cor.} = \text{FEW}, \text{ISR}, \text{ISR} + \text{FEW} \tag{14}$$

are plotted in Fig. 4. The dashed line shows the relative factorizable EW correction. The correction is small and positive a few GeV above the $t\bar{t}$-pair production threshold, but already about 20 GeV above the threshold it becomes negative and it falls down logarithmically, due to the large logarithmic terms $\sim \left[\ln\left(m_W^2/s\right)\right]^2$ and $\sim \ln\left(m_W^2/s\right)$, toward more and more negative values, reaching 20% at $\sqrt{s} = 2$ TeV. The dotted line shows the relative ISR

correction, which on the other hand is dominated by large collinear logarithms $\left[\ln\left(s/m_e^2\right)\right]^2$ and $\ln\left(s/m_e^2\right)$. It starts from the value of about -25% at energies close to the threshold and grows to almost $+25\%$ at $\sqrt{s} = 2$ TeV. Finally, the solid line shows the combined ISR and factorizable EW correction. The net relative correction is dominated by the ISR: it is large and negative for energies not far above the threshold and it becomes positive at high energies, reaching 1.4% at $\sqrt{s} = 2$ TeV.

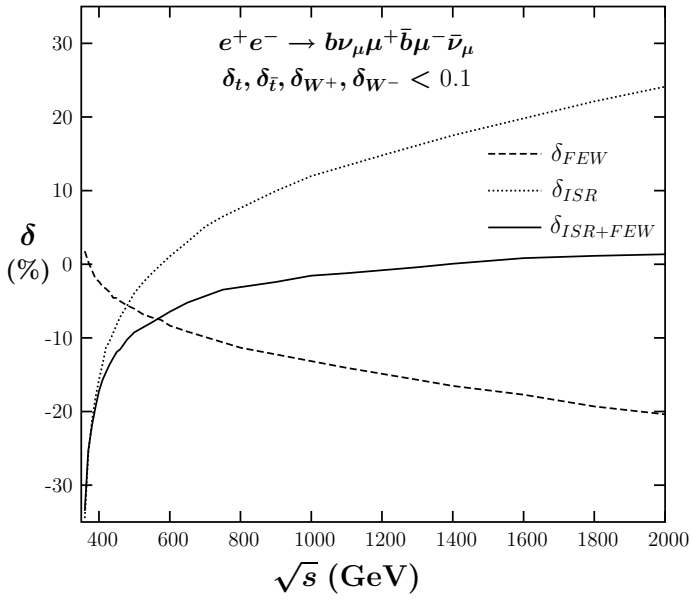

Fig. 4. Relative corrections for reaction (12) corresponding to plots in Fig. 3 as functions of the CMS energy.

In Fig. 5, we illustrate to which extent cuts on the relative departures of the invariant masses of (9) and (10) from m_t and m_W of (11) reduce the signal cross section of reaction (12). The plots in Fig. 5 show the lowest order signal cross section of (12), *i.e.* the cross section obtained with the two 'signal' Feynman diagrams of Fig. 1(a), as a function of the CM energy: the solid line shows the cross section without any cuts, the dashed-dotted line shows the cross section in the presence of cuts (13) and the dotted line the cross section with only the cuts on invariant masses of the top- and antitop-quark $\delta_t < 0.1$ and $\delta_{\bar{t}} < 0.1$. We see that the reduction of signal caused by the invariant mass cuts is not dramatic.

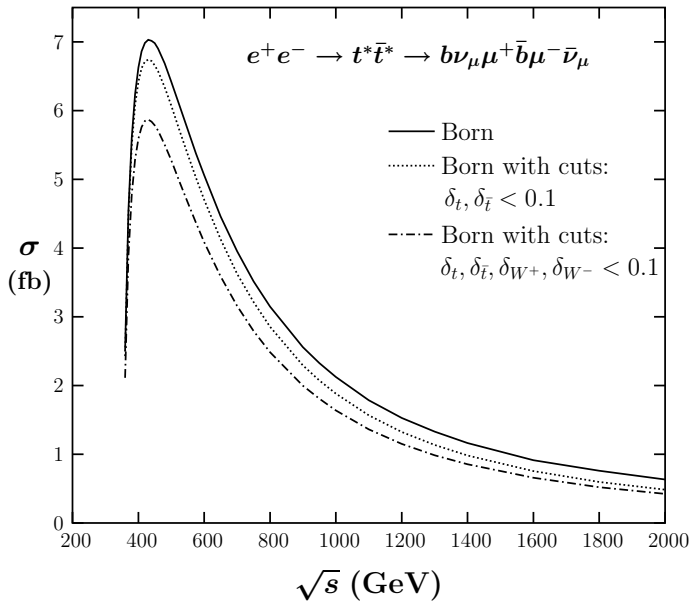

Fig. 5. "Signal" cross sections of reaction (12), as functions of the CMS energy, without cuts and with cuts on the invariant masses of the top quarks and both on the top-quarks and W-bosons.

4. Summary

We have discussed an influence of the quantum electrodynamics corrections due to the ISR in the structure function approach and factorizable EW $\mathcal{O}(\alpha)$ corrections in the pole approximation on the standard model predictions for the top quark pair production and decay into six fermions at the ILC. The corrections, which have been illustrated with numerical results for one selected six-fermion reaction (2), are quite sizeable and should be taken into account in the analysis of the future precision data. Moreover, we have illustrated how cuts on departures of invariant masses of the top-quarks and W-bosons, which are necessary in order to make the pole approximation meaningful, reduce the $t\bar{t}$ signal cross section. The reduction is not dramatic and the high precision study of the top-quark pair production should be possible at the ILC.

REFERENCES

[1] J.A. Aguilar-Saavedra *et al.* [ECFA/DESY LC Physics Working Group Collaboration], [hep-ph/0106315]; T. Abe *et al.*, [American Linear Collider Working Group Collaboration], SLAC-R-570 [hep-ex/0106056]; K. Abe *et al.* [ACFA Linear Collider Working Group Collaboration], hep-ph/0109166.

[2] A. Biernacik, K. Kołodziej, A. Lorca, T. Riemann, *Acta Phys. Pol. B* **34**, 5487 (2003) [hep-ph/0311097].

[3] K. Kołodziej, A. Staroń, A. Lorca, T. Riemann, hep-ph/0510195.

[4] K. Kołodziej, *Eur. Phys. J.* **C23**, 471 (2002) [hep-ph/0110063].

[5] A. Biernacik, K. Kołodziej, *Nucl. Phys. Proc. Suppl.* **116**, 33 (2003) [hep-ph/0210405].

[6] K. Kołodziej, *Acta Phys. Pol. B* **34**, 4511 (2003).

[7] W. Beenakker, F.A. Berends, A.P. Chapovsky, *Nucl. Phys.* **B548**, 3 (1999); A. Denner, *et al.*, *Nucl. Phys.* **B587**, 67 (2000); S. Jadach *et al.*, *Phys. Rev.* **D61**, 113010 (2000).

[8] F. Jegerlehner, K. Kołodziej, T. Westwański, *Eur. Phys. J.* **C44**, 195 (2005); hep-ph/0503169.

[9] W. Beenakker *et al.*, in G. Altarelli, T. Sjöstrand, F. Zwirner (eds.), Physics at LEP2 (Report CERN 96-01, Geneva, 1996), Vol. 1, p. 79 [hep-ph/9602351].

[10] K. Kołodziej, *Comput. Phys. Commun.* **151**, 339 (2003) [arXiv:hep-ph/0210199].

[11] J. Fleischer, A. Leike, T. Riemann, A. Werthenbach, *Eur. Phys. J.* **C31**, 37 (2003) [hep-ph/0302259]; J. Fleischer, A. Leike, A. Lorca, T. Riemann, A. Werthenbach, Fortran program topfit v.0.93 (10 Jun 2003); available at http://www-zeuthen.desy.de/theory/research; A. Lorca, T. Riemann, hep-ph/0412047, to appear in *Comput. Phys. Commun.*; A. Lorca, DESY-THESIS-2005-004.

[12] B. Grządkowski *et al.*, *Nucl. Phys.* **B281**, 18 (1987); W. Beenakker, S.C. van der Marck, W. Hollik, *Nucl. Phys.* **B365**, 24 (1991); R.J. Guth, J.H. Kühn, *Nucl. Phys.* **B368**, 38 (1992); W. Beenakker, A. Denner, A. Kraft, *Nucl. Phys.* **B410**, 219 (1993); V. Driesen, W. Hollik, A. Kraft, hep-ph/9603398, in e^+e^- Collisions at TeV Energies: The Physics Potential, Proceedings of the Workshop, Annecy, Gran Sasso, Hamburg, February 1995–September 1995, edited by P.M. Zerwas, DESY 96–123D, (1996) 33; A.A. Akhundov, D.Yu. Bardin, A. Leike, *Phys. Lett.* **B261**, 321 (1991).

[13] J. Fleischer, J. Fujimoto, T. Ishikawa, A. Leike, T. Riemann, Y. Shimizu, A. Werthenbach, in KEK Proceedings 2002-11 (2002) (ed. Y. Kurihara), p. 153, hep-ph/0203220; T. Hahn, W. Hollik, A. Lorca, T. Riemann, A. Werthenbach, hep-ph/0307132.

[14] M. Jeżabek, J.H. Kühn, *Nucl. Phys.* **B314**, 1 (1989); G. Eilam, R.R. Mendel, R. Migneron, A. Soni, *Phys. Rev. Lett.* **66**, 3105 (1991); A. Denner, T. Sack, *Nucl. Phys.* **B358**, 46 (1991); A. Denner, *Fortschr. Phys.* **41**, 307 (1993); A. Czarnecki, K. Melnikov, *Nucl. Phys.* **B544**, 520 (1999); K.G. Chetyrkin, R. Harlander, T. Seidensticker, M. Steinhauser, *Phys. Rev.* **D60**, 114015 (1999).

[15] D. Bardin, S. Riemann, T. Riemann, *Z. Phys.* **C32**, 121 (1986); F. Jegerlehner, in *"Proc. of the XI International School of Theoretical Physics"*, ed. M. Zrałek and R. Mańka, World Scientific, 1988, pp. 33–108; A. Denner, T. Sack, *Z. Phys.* **C46**, 653 (1990).